Osteoarthritis and Cartilage 21 (2013) 614–624

Osteoarthritis and Cartilage

Parathyroid hormone [1-34] improves articular cartilage surface architecture and integration and subchondral bone reconstitution in osteochondral defects *in vivo*

P. Orth †‡, M. Cucchiarini †, D. Zurakowski §, M.D. Menger ||, D.M. Kohn ‡, H. Madry †‡*

† *Center of Experimental Orthopaedics, Saarland University, Homburg/Saar, Germany*
‡ *Department of Orthopaedic Surgery, Saarland University Medical Center, Homburg/Saar, Germany*
§ *Department of Orthopedic Surgery, Boston Children's Hospital, Harvard Medical School, Boston, MA, USA*
|| *Institute for Clinical and Experimental Surgery, Saarland University Medical Center, Saarland University, Homburg/Saar, Germany*

ARTICLE INFO

Article history:
Received 1 October 2012
Accepted 12 January 2013

Keywords:
PTH [1-34]
PTH1R
Osteochondral defect
Cartilage repair
Subchondral bone

SUMMARY

Objective: The 1-34 amino acid segment of the parathyroid hormone (PTH [1-34]) mediates anabolic effects in chondrocytes and osteocytes. The aim of this study was to investigate whether systemic application of PTH [1-34] improves the repair of non-osteoarthritic, focal osteochondral defects *in vivo*.
Design: Standardized cylindrical osteochondral defects were bilaterally created in the femoral trochlea of rabbits ($n = 8$). Daily subcutaneous injections of 10 μg PTH [1-34]/kg were given to the treatment group ($n = 4$) for 6 weeks, controls ($n = 4$) received saline. Articular cartilage repair was evaluated by macroscopic, biochemical, histological and immunohistochemical analyses. Reconstitution of the subchondral bone was assessed by micro-computed tomography. Effects of PTH [1-34] on synovial membrane, apoptosis, and expression of the PTH receptor (PTH1R) were determined.
Results: Systemic PTH [1-34] increased PTH1R expression on both, chondrocytes and osteocytes within the repair tissue. PTH [1-34] ameliorated the macro- and microscopic aspect of the cartilaginous repair tissue. It also enhanced the thickness of the subchondral bone plate and the microarchitecture of the subarticular spongiosa within the defects. No significant correlations were established between these coexistent processes. Apoptotic levels, synovial membrane, biochemical composition of the repair tissue, and type-I/II collagen immunoreactivity remained unaffected.
Conclusions: PTH [1-34] emerges as a promising agent in the treatment of focal osteochondral defects as its systemic administration simultaneously stimulates articular cartilage and subchondral bone repair. Importantly, both time-dependent mechanisms of repair did not correlate significantly at this early time point and need to be followed over prolonged observation periods.

Introduction

Osteochondral defects critically affect the articular cartilage and the underlying subchondral bone[1]. Due to their intimate cross-talk[2,3], both components of the osteochondral unit need to be addressed therapeutically[4]. Established reconstructive surgical therapies include osteochondral transplantation[5] or subchondral bone grafts combined with autologous chondrocyte implantation[6,7]. However, problems such as donor-site morbidity[8] and disturbed remodeling of the osteochondral unit[6,9] are unsolved issues. Moreover, there are currently no systemic or local non-surgical options available for addressing the problem of limited osteochondral repair in non-osteoarthritic cartilage defects.

Parathyroid hormone (PTH) is anabolic for osteocytes[10] and chondrocytes[11] and its actions are mediated by the PTH receptor (PTH1R)[12]. The 1-34 amino acid segment of PTH (PTH [1-34])[13] is approved for the systemic treatment of postmenopausal osteoporosis[14]. Recent experimental data suggest that PTH [1-34] also enhances fracture repair[15] and spinal fusion[16] *in vivo*. It further inhibits the progression of osteoarthritis in mice[17] and rats[18], and intraarticular application of the full-length PTH [1-84] molecule *via* osmotic pumps over several weeks advanced the repair of shallow chondral defects *in vivo*[19].

It remains unknown, however, whether PTH [1-34] is capable of simultaneously stimulating the restoration of the subchondral bone

* Address correspondence and reprint requests to: H. Madry, Center of Experimental Orthopaedics, Saarland University, Kirrberger Strasse, Building 37-38, D-66421 Homburg/Saar, Germany. Tel: 49-6841-1624590; Fax: 49-6841-1624569.
E-mail addresses: patrick.orth@uks.eu (P. Orth), mmcucchiarini@hotmail.com (M. Cucchiarini), david.zurakowski@childrens.harvard.edu (D. Zurakowski), michael.menger@uks.eu (M.D. Menger), dieter.kohn@uks.eu (D.M. Kohn), henning.madry@uks.eu (H. Madry).

1063-4584/$ – see front matter
http://dx.doi.org/10.1016/j.joca.2013.01.008

and the articular cartilage in focal osteochondral defects. Here, we tested the hypothesis that prolonged subcutaneous application of PTH [1-34] improves the reconstitution of the entire osteochondral unit in a translational rabbit osteochondral defect model. We further hypothesized that the degree of subchondral bone reconstitution correlates with articular cartilage repair *in vivo*.

Materials and methods

Animal experiments

All animal procedures were approved by the local Governmental Animal Care Committee. Female Chinchilla bastard rabbits in their late juvenile stage ($n = 8$; Charles River, Sulzfeld, Germany; mean body weight (BW): 3.1 kg (3.0, 3.2); mean age: 14 weeks (12, 16)) were anesthetized by intramuscular injection of Rompun (0.2 ml/kg BW; Bayer, Leverkusen, Germany) and Ketavet (0.75 mg/kg BW; Pharmacia & Upjohn, Erlangen, Germany). The knee joint was entered as previously described[1]. Two standardized cylindrical osteochondral defects (diameter 3.2 mm, depth 5.0 mm) were created in the patellar groove of each knee ($n = 32$ defects) with a manual cannulated burr with a flat tip (Synthes, Umkirch, Germany) and a custom made drill stop as previously described[1]. The defects were washed with PBS (phosphate buffered saline), the patella was reduced and the incisions were closed in layers.

Postoperatively, the eight animals were randomly divided into two groups: the treatment group (PTH group; $n = 4$) received once daily (18:00 h) subcutaneous injections of 10 μg/kg BW of human PTH [1-34] (Bachem, Bubendorf, Switzerland; 74% homology with lapine PTH [1-34]) dissolved in 0.5 M saline with 2% heat inactivated bovine serum (BS) over 42 days (Table I). Control animals ($n = 4$) were daily injected with 0.5 M saline with 2% heat inactivated BS only. The animals were allowed immediate full weight bearing and were fed a standard diet. No postoperative analgesia was administered. Two joints were excluded from further analyses because of macroscopic signs of infection. Blood samples were collected at days 0, 21, and 42 from all animals and analyzed for serum levels of calcium and alkaline phosphatase (AP).

After 6 weeks, the rabbits were euthanized with pentobarbital (150 mg/kg BW; Merial, Hallbergmoos, Germany) and the defects were photo documented for macroscopic assessment under standardized illumination conditions[20]. The entire cartilaginous repair tissue of the proximal defects was retrieved ($n = 14$) and stored at −80°C for biochemical analysis. The remaining distal femurs ($n = 14$) were dissected and fixed in 4% phosphate buffered formalin.

Macroscopic assessment of the joints

Based on the photographs taken immediately after sacrifice, the defect areas ($n = 14$) were examined macroscopically in a blinded fashion. An inverse scoring system[20] was applied, incorporating individual parameters for color and surface of the repair tissue, presence of blood vessels, filling of the defect and integrity of the adjacent articular cartilage. The individual scores (0–4 points for each parameter) were combined, resulting in an average total score ranging from 20 points (no signs of repair) to 0 points (normal articular cartilage)[20].

Micro-computed tomography analysis of the subchondral bone

All trochleas ($n = 7$ per group) were scanned within 70% ethanol at a spatial resolution of 13 μm in a microfocused X-ray CT scanner (μCT; Skyscan 1172, Skyscan, Kontich, Belgium) with the tube voltage set at 70 kV and the current at 140 μA. Projections (1,100–1,300 per specimen) were obtained at 0.4° intervals with 2,400-ms exposure time and a combined 0.5 mm aluminium/copper filter interposed. Frontal sections were reconstructed by a modified Feldkamp cone-beam algorithm[21] (NRecon, Skyscan). Thresholding levels of gray values (range 89–255) were set for segmentation of binary images. To express gray values as mineral content (bone mineral density; BMD), calcium hydroxyapatite (CaHA) phantom rods with known BMD values (250 and 750 mg CaHA/cm^3) were employed for calibration.

Based on the estimated original size of the cylindrical defects (3.2 × 5.0 mm), standardized dimensions of 3.0 mm in width (frontal plane) and length (sagittal plane) were set for all six volumes of interest (VOIs; Fig. 1). Within the defects, the VOI "defect subchondral bone plate" (defect SBP) involved exclusively the SBP, "defect subarticular spongiosa" (defect SAS) was located within trabecular bone. The total depth of both VOIs did not exceed 4.0 mm. The VOIs "lateral adjacent SBP" (lateral SBP) and "medial adjacent SBP" (medial SBP) were placed within the neighboring SBPs. Beneath lateral and medial SBP, lateral and medial SAS adjoined. Overlapping of individual VOIs was avoided (Fig. 1). For data presentation, the VOIs medial and lateral SBP as wells as medial and lateral SAS were combined, resulting in the virtual VOIs adjacent SBP and adjacent SAS, respectively. In one untreated animal ($n = 2$ femurs), parameters of normal SBP and SAS were determined.

BMD, bone volume fraction (BV/TV), bone surface/volume ratio (BS/BV), and bone surface density (BS/TV) were computed in a direct 3-dimensional fashion in all VOIs (CT Analyzer, Skyscan). Cortical thickness (Ct.Th) was evaluated only within the SBP, while trabecular thickness (Tb.Th), trabecular separation (Tb.Sp), trabecular pattern factor (Tb.Pf), trabecular number (Tb.N), structure model index (SMI), degree of anisotropy (DA), and fractal dimension (FD) were assessed in the SAS[21].

Biochemical evaluation of the repair tissue

Repair tissue retrieved from the proximal defects was thawed and digested overnight in 100 μl 0.0125% papain solution at 60°C. Digested samples were processed (GENios; Tecan, Crailsheim,

Table I
Study design. Two standardized osteochondral defects (proximal and distal) were established bilaterally in each trochlea of rabbits ($n = 8$ animals; $n = 32$ defects). The treatment group ($n = 4$ animals) received daily subcutaneous injections of 10 μg PTH [1-34] per kg BW for 6 weeks[16]. The control group received daily injections of saline. In each group, one joint had to be excluded from further analysis due to infection. After 6 weeks, both components of the osteochondral unit were simultaneously analyzed: reconstitution of the subchondral bone was assessed by micro-computed tomography. Articular cartilage repair was evaluated by macroscopic, biochemical, histological and immunohistochemical analyses of the distal defects as well as by biochemical assessment of the repair tissues derived from the proximal defects within each joint. The effect of PTH [1-34] on synovial membrane, apoptosis, and PTH1R expression on osteocytes and chondrocytes was determined

Group	Number of animals	Number of joints analyzed	Number of joints infected	Number of defects analyzed	Subcutaneous application	Treatment period
PTH [1-34]	4	7	1	14	Daily	6 Weeks
Control (saline)	4	7	1	14	Daily	6 Weeks

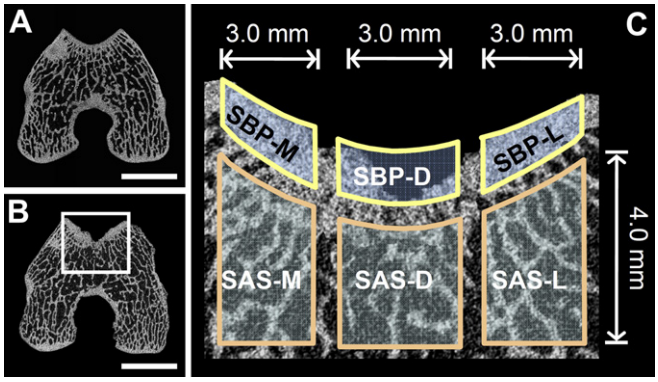

Fig. 1. Evaluation of subchondral bone changes by micro-computed tomography. Overview of a frontal μCT section of the distal femur at the level of the trochlear groove from a non-operated rabbit (A) and 6 weeks after the creation of an osteochondral defect (B). The μCT analysis was performed applying the VOIs displayed in image (C), which represents a magnified view of the area indicated in image (B). SBP-D/SAS-D: osteochondral defect areas, SBP-M/SAS-M: medial to the defects, SBP-L/SAS-L: lateral to the defects. The subchondral bone within osteochondral defects (SBP-D, SAS-D) was significantly deteriorated compared to the unaffected, adjacent bone (SBP-M/L, SAS-M/L). PTH [1-34] application significantly increased thickness of the defect SBP (SBP-D), BV/TV and BMD of the adjacent SBP (SBP-M/L), and microarchitectural parameters of defect and adjacent SAS (SAS-D, SAS-M/L; Table IV). Scale bars: 5.0 mm (A, B).

Germany) to monitor the production of proteoglycans and the DNA contents by binding to dimethylmethylene blue (DMMB) dye (Serva, Heidelberg, Germany) and by Hoechst 33258 assay (Sigma, Munich, Germany), respectively[22]. Data were normalized to total cellular proteins using a protein assay (Pierce Thermo Scientific, Schwerte, Germany).

Histological and immunohistochemical analyses

Distal femurs were trimmed, decalcified, and paraffin-embedded frontal sections (5 μm) of the distal defects were stained with safranin orange/fast green (safranin O) or haematoxylin/eosin (HE) according to routine protocols[23]. All histological scoring was performed blinded. Photomicrographs (Figs. 2–4) were obtained using a solid-state CCD camera mounted on a BX-45 microscope (Olympus, Hamburg, Germany).

The synovial membrane was evaluated on HE-stained sections ($n = 14$) using a previously published scoring system[24]. The three categories in this system include villus thickening (fibrosis), villus architecture (blunting) and the presence of inflammatory cell infiltrates. Total point values range between 0 and 9 points.

Visualization of the collagen network (birefringence, orientation, and anisotropy) within the repair tissue was performed using polarized light microscopy.

Immunostaining was performed as previously described[25] using a 1/50 dilution of a monoclonal mouse anti-type-I or anti-type-II collagen IgG (both Acris, Hiddenhausen, Germany), a cleaved caspase-3 polyclonal antibody (Asp175; Cell Signaling Technology, Frankfurt, Germany), or a monoclonal mouse PTH1R antibody (ab3271; Abcam, Cambridge, UK), and a secondary biotinylated anti-mouse antibody (Vector Laboratories, Grünberg, Germany). Immunoreactivity to type-I collagen in the repair tissue was compared with that of the adjacent subchondral bone, serving as a positive internal control. Immunoreactivity to type-II collagen in the repair tissue was compared with that of the adjacent articular cartilage. A score was given to each knee with 0 points indicating no immunoreactivity; 1: significantly weaker; 2: moderately weaker; 3: similar, and 4: stronger immunoreactivity compared with the internal controls. Immunoreactivity to both collagens was also compared with normal lapine articular cartilage. For the evaluation of caspase-3 immunostaining, images of the histological sections taken at 200-fold magnification were digitalized and six standardized regions of interest (ROIs; 0.1 mm^2) were defined within and adjacent to the defects in the superficial cartilage layer (apical half), the deep cartilage layer (basal half) and the subchondral bone (analySIS docu 5.0, Olympus Soft Imaging Solutions, Münster, Germany). Total cell numbers and apoptosis rates were determined histomorphometrically (Table II). PTH1R expression was determined as the percentage of stained cells in six standardized ROIs (0.1 mm^2 each) within repair cartilage and repair subchondral bone. Two sections were scored per defect and antibody.

Degenerative changes in the articular cartilage adjacent to the defects were evaluated within a 3 mm area neighboring both integration sides (excluding the area of integration) on safranin O-stained sections, applying the scoring system for osteoarthritic lapine cartilage of Laverty *et al.*[26] (Table III).

For quantitative assessment of the repair tissue, serial histological sections of the distal femora were taken at 200 μm intervals. Safranin O-stained sections within approximately 1.0 mm from the center of the defect ($n = 8–10$ per defect) were analyzed using the simple articular cartilage repair scoring system according to Wakitani *et al.*[27] and the complex score described by Sellers *et al.*[28,29] (Table III). A total of 116 sections were scored twice by one blinded investigator.

Correlation between articular cartilage and subchondral bone repair

Correlations between the histological total average point values and the key μCT parameters BMD, BV/TV and Ct.Th or Tb.Th from VOIs comprising deteriorated cortical (defect SBP) and trabecular (defect SAS) subchondral bone were determined.

Statistical analysis

Each test condition was performed with $n = 4$ independent animals ($n = 7$ joints) per group. Since the data involve multiple observations on different joints from the same animals, these are likely positively correlated when compared to observations from a different animal. In order to obtain mean comparisons in the context of a model that takes into account these correlations, we employed a linear model using generalized estimating equations (GEE) with an exchangeable working correlation structure (which with no more than two observations per animal, is an entirely general structure). Standard errors were based on a robust estimated covariance matrix (Huber-White or "sandwich" estimator). The Bland–Altman method for calculating weighted correlation coefficients (r) between subjects with repeated observations[30] was used to determine the strength of association between the histological average total scores[27,28] and key μCT parameters. Based on sample sizes and differences in μCT parameters of subchondral bone, a power of 80% for detecting large treatment effects (approximately 1.3–1.5 standard deviations) was achieved. Data are presented as mean values, 95% confidence intervals are used to denote statistical uncertainty of estimates and are given in parentheses. Two-tailed values of $P < 0.05$ were considered significant. Statistical analyses were performed using the SPSS software package (version 19.0, SPSS Inc./IBM, Chicago, IL).

Results

Effect of systemic PTH [1-34] application on PTH1R expression

PTH [1-34] induced a consecutive up-regulation of PTH1R expression on both, osteocytes within the repaired subchondral

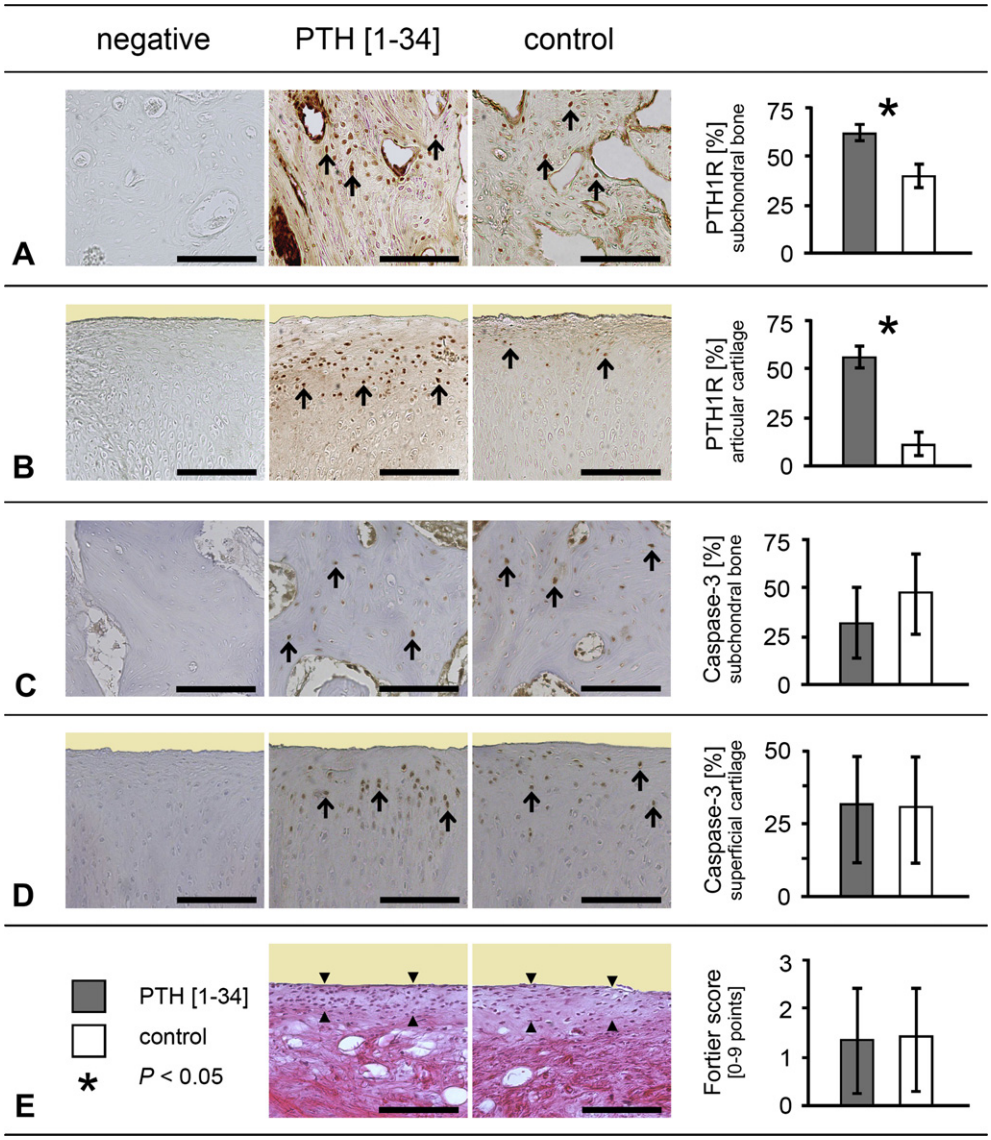

Fig. 2. PTH1R expression in osteochondral defects and exclusion of potential deleterious responses following systemic PTH [1-34] administration *in vivo*. Prolonged PTH [1-34] treatment induced an up-regulation of PTH1R expression on both, osteocytes within the subchondral bone (A) and chondrocytes of the articular cartilage (B) from osteochondral defect areas. This simultaneous response of both cell populations constituting the osteochondral unit might explain the coexistent improvement of articular cartilage and subchondral bone repair in osteochondral defects by PTH [1-34]. The treatment neither induced an increase in the apoptosis rate of osteocytes (C) and chondrocytes (D) within the repair tissue nor an inflammatory response in the synovial membrane (E). Arrowheads (A–D) point at some of the immunopositive cells. Sections were taken from defects having a histological rating equal to the mean score for its respective treatment group. Negative controls (left images in A–D) show immunostainings with omission of the primary antibody. Triangles in (E) delimit the thickness of the apical layer of the synovial membrane which overlies a stroma of loose soft tissue rich in collagen fibers and adipocytes. Graphs indicate mean values and 95% confidence intervals (error bars) based on $n = 4$ independent observations. Scale bars: 0.2 mm.

bone (64% (59, 69) vs 38% (32, 43) positive cells ($P < 0.001$)) and chondrocytes within the cartilage repair tissue (57% (51, 62) vs 9% (3, 15); $P < 0.001$; Fig. 2) when compared to controls.

Effect of PTH [1-34] on calcium and AP levels

Before PTH [1-34] administration, no differences were detected between PTH and control groups in calcium (3.53 mmol/l (3.35, 3.70) vs 3.69 mmol/l (3.29, 4.09); $P = 0.51$) and AP serum levels (80.50 U/l (74.70, 86.30) vs 76.50 U/l (62.22, 90.78); $P = 0.64$). At day 21, similar results were obtained (calcium: 3.61 mmol/l (3.58, 3.64) vs 3.48 mmol/l (3.31, 3.65): $P = 0.40$; AP: 81.00 U/l (69.91, 92.09) vs 75.00 U/l (45.90, 104.10): $P = 0.81$). However, serum levels for calcium (4.10 mmol/l (3.87, 4.32) vs 3.58 mmol/l (3.41, 3.75); $P = 0.01$) and AP (90.25 U/l (85.99, 94.51) vs 69.25 U/l (62.12, 76.38); $P = 0.004$) were significantly increased after 42 days of PTH [1-34] administration compared with controls.

Examination of potential deleterious responses to PTH [1-34]

Apoptosis rate of chondrocytes and osteocytes

Cell numbers and apoptosis rates of chondrocytes and osteocytes in different compartments of the osteochondral unit are given in Table II. Caspase-3 immunoreactivity was significantly higher in the superficial than in the deep zone of the cartilage repair tissue ($P = 0.04$). Systemic application of PTH [1-34] had no significant effect on the rate of apoptosis in any of the regions evaluated (all $P > 0.10$; Fig. 2).

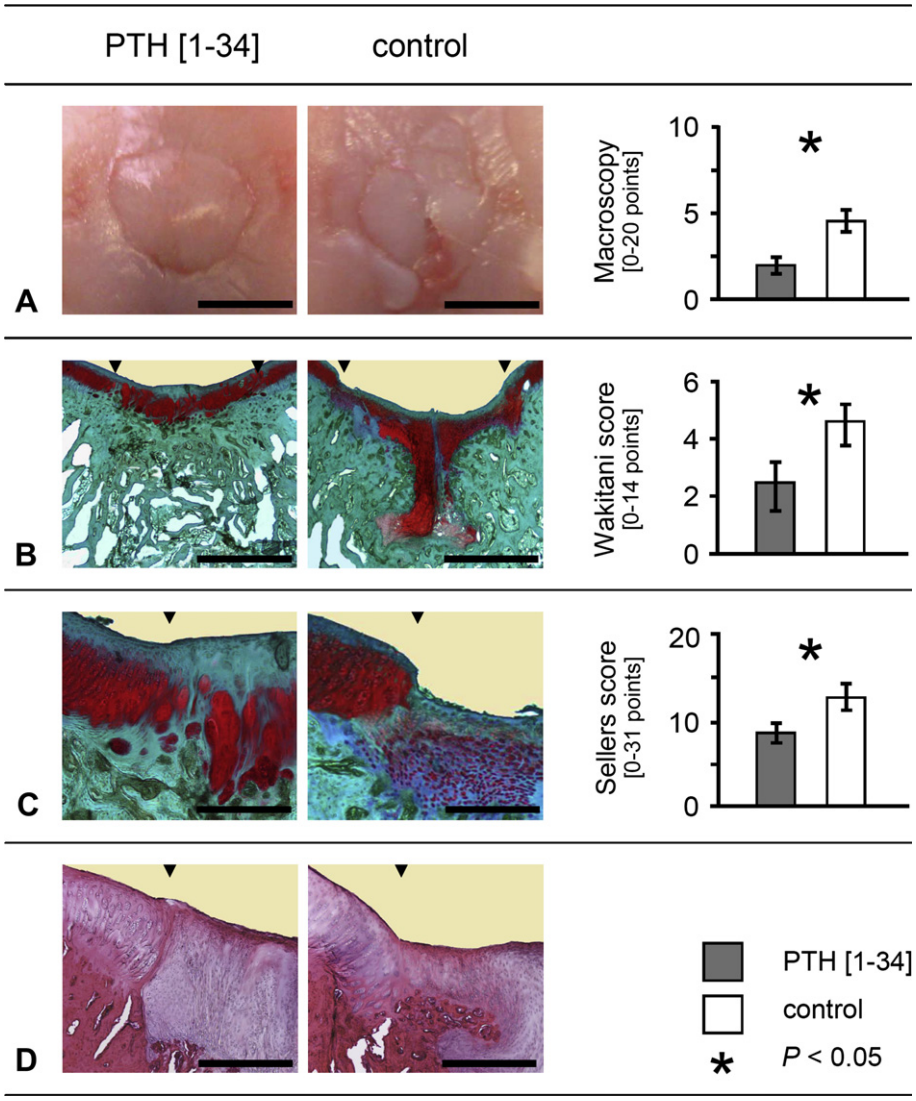

Fig. 3. Macroscopic and histological assessment of articular cartilage repair following systemic PTH [1-34] application *in vivo*. Compared to controls, treatment with PTH [1-34] significantly improved the macroscopic appearance[20] of the articular cartilage repair tissue (A). This improvement was also reflected in the histological evaluation following staining with safranin O (B, C) or HE (D), applying either a simple[27] (B) or a complex[28] (C) scoring system. Sections were taken from defects having a histological rating equal to the mean score for its respective treatment group. Margins of the defects are denoted by black triangles. Graphs indicate mean values and 95% confidence intervals (error bars) based on $n = 4$ independent observations. Scale bars: 5.0 mm (A), 2.0 mm (B), or 1.0 mm (C, D).

Inflammatory reaction of the synovial membrane

According to the applied scoring system[24], there were no differences (all $P > 0.70$) in the thickness (mean score 0.3 (0.1, 0.6) vs 0.4 (0.1, 0.6)) or architecture (0.6 (0.1, 1.1) vs 0.5 (0, 1.0)) of synovial villi or in the presence of inflammatory cell infiltrates (0.4 (0, 0.8) vs 0.3 (0, 0.7)) between knees of the PTH group and control joints (Fig. 2). The average total scores were comparatively low for both groups (1.3 (0.1, 2.4) vs 1.3 (0.2, 2.5); $P = 0.95$), indicating the lack of synovial changes induced by systemic PTH [1-34].

Effect of PTH [1-34] on articular cartilage repair

Macroscopic evaluation

After 6 weeks *in vivo*, systemic PTH [1-34] application yielded a significant transformation of the color of the repair tissue[20] from white to hyaline (1.1 (0.9, 1.4) vs 0.1 (0, 0.4); $P < 0.001$), and improved the defect surface (1.0 (1.0, 1.0) vs 1.7 (1.7, 1.7; $P < 0.001$)) and the average total score (2.1 (1.9, 2.4) vs 4.7 (4.4, 4.9); $P < 0.001$; Fig. 3) compared to controls.

Biochemical characterization of the cartilaginous repair tissue

Systemic PTH [1-34] application did not affect the ratio of proteoglycan per protein mass (0.06 μg/μg (0.04, 0.09) vs 0.07 μg/μg (0.04, 0.10); $P = 0.69$) and DNA per protein mass (16.31 ng/μg (7.21, 25.40) vs 22.20 ng/μg (13.10, 31.29); $P = 0.37$) within the repair tissues. The ratio of proteoglycan per DNA remained consistently low irrespective of whether the tissues were exposed to PTH [1-34] or not (0.01 μg/ng (0, 0.02) vs 0 μg/ng (0, 0.01); $P = 0.26$).

Degenerative changes in the adjacent articular cartilage

PTH [1-34] application led to a significantly increased formation of clusters (chondrons; $P = 0.03$) in the adjacent cartilage. However, the average total score of cartilage degradation[26] remained unchanged between PTH and control group (Table III).

Histological grading of articular cartilage repair

Applying the elementary Wakitani score[27] to evaluate cartilage repair, PTH [1-34] administration significantly improved surface regularity (3.3-fold) and integration of the cartilaginous repair

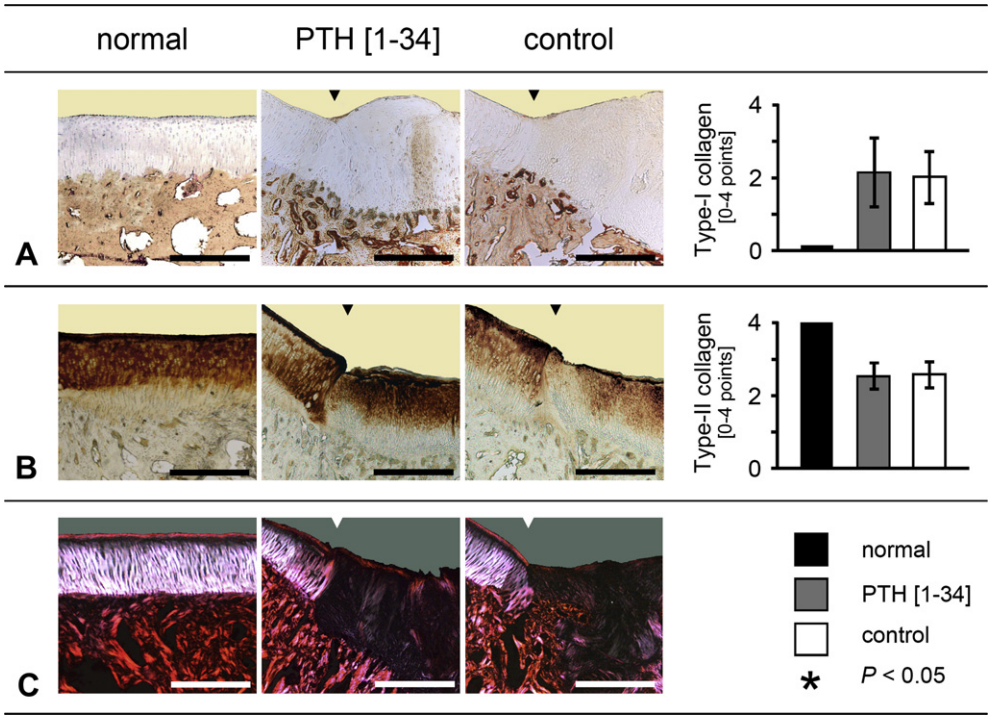

Fig. 4. Collagen distribution within the osteochondral unit. PTH [1-34] did not provoke changes in the immunoreactivity to a monoclonal mouse anti-human type-I collagen IgG (A) or to a monoclonal mouse anti-human type-II collagen IgG (B) at this early time point of 6 weeks after defect creation. In both groups, collagen fibrils within the repair tissue did not reproduce a normal articular cartilage organization, but birefringence of the subchondral bone was similar between defects and the adjacent bone (C). Sections were taken from defects having a histological rating equal to the mean score for its respective treatment group. Normal controls (left images in A–C) show the intact osteochondral unit of a non-operated lapine trochlear groove. Margins of the defects are denoted by triangles. Graphs indicate mean values and 95% confidence intervals (error bars) based on $n = 4$ independent observations. Scale bars: 1.0 mm.

tissue (2.0-fold) after 6 weeks (Table III). The average total score value was significantly improved following treatment with PTH [1-34] ($P < 0.001$; Fig. 3).

When the complex histological scoring system of Sellers *et al.*[28] was used, the individual parameters of integration (1.3-fold), matrix staining (8.3-fold), and defect as well as surface architecture (2.2-fold and 1.8-fold, respectively) were significantly improved in the PTH group (all $P < 0.05$; Table III). Importantly, the average total score was significantly improved by PTH [1-34] ($P < 0.001$; Fig. 3), and highly correlated with the Wakitani total score ($r = 0.978$ (0.878–0.996); $P < 0.001$).

Distribution of collagens within the osteochondral unit

Polarized light microscopy

Polarized light microscopic assessment revealed that collagen fibrils within the repair tissue of both groups did not reproduce a normal articular cartilage organization. Irrespective of the treatment, birefringence (an indicator of collagen content) was always weaker within the repair tissues than in the surrounding cartilage (Fig. 4). Birefringence of the subchondral bone was similar between the defect areas and the adjacent tissue in both groups.

Type-I and type-II collagen immunostaining

At this early time point, immunoreactivity to type-I collagen was similar in the cartilage repair tissue of animals from the PTH group (mean score 2.4 (1.5, 3.3)) and the control group (2.0 (1.1, 2.9); $P = 0.57$). Between both groups, no differences were detected for the presence of type-II collagen in the cartilage repair tissues, a major component of hyaline articular cartilage (2.6 (2.4, 2.9) vs 2.7 (2.5, 3.0); $P = 0.64$; Fig. 4).

Effect of PTH [1-34] on the microarchitecture of the subchondral bone

Evaluation of adjacent subchondral bone

PTH [1-34] enhanced BV/TV and BMD as well as Ct.Th of the adjacent SBP (Table IV). Simultaneously, PTH [1-34] enhanced Tb.Th

Table II
Cell numbers and apoptosis rates in different compartments of the osteochondral unit. Caspase-3 immunoreactivity was evaluated in six standardized ROIs (0.1 mm^2 each) within and adjacent to the osteochondral defects in the superficial cartilage layer (apical half), the deep cartilage layer (basal half), and the subchondral bone. Apoptosis rates were higher for chondrocytes in the superficial than in the deep zone of the cartilage repair tissue. Systemic application of PTH [1-34] had no significant effect on total cell numbers and on the rate of apoptosis in any of the regions evaluated

Region	Total cell number			Apoptosis rate		
	PTH [1-34]	Control	*P*	PTH [1-34]	Control	*P*
Defect: superficial cartilage	114.8 (95.4, 134.1)	147.5 (114.1, 180.9)	0.16	29.5 (10.3, 48.7)	28.8 (9.6, 48.0)	0.96
Defect: deep cartilage	113.5 (84.7, 142.3)	148.0 (121.0, 175.0)	0.20	0 (0, 0.4)	0.5 (0.1, 0.9)	0.11
Defect: subchondral bone	79.8 (58.4, 101.1)	102.5 (60.6, 144.4)	0.40	30.1 (9.3, 50.9)	46.7 (26.0, 67.5)	0.27
Adjacent: superficial cartilage	105.5 (97.5, 113.5)	96.8 (88.3, 105.2)	0.19	2.1 (0, 14.3)	12.9 (0.7, 25.2)	0.22
Adjacent: deep cartilage	81.3 (66.6, 95.9)	95.8 (82.6, 108.9)	0.20	5.7 (0.3, 11.1)	8.8 (3.3, 14.2)	0.44
Adjacent: subchondral bone	69.0 (50.1, 87.9)	91.8 (74.4, 109.1)	0.11	22.5 (3.3, 41.6)	23.1 (13.0, 33.1)	0.95

Table III
Applied inverse histological grading systems and obtained score values for the histological evaluation of the adjacent articular cartilage[26] and the cartilaginous repair tissues[27,28]. Effect of PTH [1-34] application on the histological grading of the adjacent articular cartilage (Laverty[26] score) and the cartilage repair tissue (Wakitani[27] and Sellers[28] scores) at 6 weeks *in vivo*. Mean values and 95% confidence intervals represent the estimated scores in points for each category and the average total scores; lower point values indicate a better histological appearance of the tissue. PTH [1-34] administration did not affect degenerative changes in the adjacent articular cartilage. The treatment improved all individual parameters of the repair tissues in both scores and significantly improved the total average scores (both $P < 0.05$), indicating a better quality of the cartilage repair tissue following PTH [1-34] administration. Statistical significance is highlighted by bold letters

	Assignable point values	PTH [1-34]	Control	X-fold	*P*
Laverty score[26]					
Matrix staining	(0–6)	3.79 (2.42, 5.17)	4.35 (2.98, 5.73)	0.87	0.57
Structure	(0–11)	2.84 (1.09, 4.60)	1.78 (0.02, 3.53)	1.60	0.40
Chondrocyte density	(0–4)	1.86 (0.61, 3.12)	1.84 (0.58, 3.09)	1.01	0.98
Cluster formation	(0–3)	1.96 (1.58, 2.35)	1.35 (0.97, 1.74)	1.45	**0.03**
Average total score	*(0–24)*	*10.18 (6.22, 14.14)*	*9.22 (5.26, 13.18)*	*1.10*	*0.74*
Wakitani score[27]					
Cell morphology	(0–4)	0.97 (0.80, 1.14)	1.13 (0.97, 1.31)	1.16	0.18
Matrix staining	(0–3)	0.13 (0, 0.43)	0.32 (0.02, 0.61)	2.46	0.39
Surface regularity	(0–3)	0.62 (0.06, 1.18)	2.06 (1.50, 2.62)	3.32	**<0.001**
Thickness	(0–2)	0 (0, 0)	0 (0, 0)	1.00	n.a.
Integration	(0–2)	0.44 (0.27, 0.62)	0.86 (0.68, 1.03)	1.95	**0.001**
Average total score	*(0–14)*	*2.17 (1.36, 2.98)*	*4.37 (3.56, 5.19)*	*2.01*	***<0.001***
Sellers score[28]					
Filling of defect	(0–4)	0 (0, 0.17)	0.21 (0.04, 0.37)	n.a.	0.09
Integration	(0–3)	1.44 (1.22, 1.67)	1.90 (1.68, 2.13)	1.32	**0.01**
Matrix staining	(0–4)	0.04 (0, 0.24)	0.33 (0.14, 0.53)	8.25	**0.04**
Cell morphology	(0–5)	1.99 (1.64, 2.33)	2.21 (1.86, 2.55)	1.11	0.38
Architecture (defect)	(0–4)	0.64 (0.33, 0.96)	1.41 (1.10, 1.72)	2.20	**0.001**
Architecture (surface)	(0–3)	1.18 (0.71, 1.65)	2.06 (1.59, 2.53)	1.75	**0.01**
Subchondral bone	(0–4)	0.27 (0, 0.79)	0.98 (0.47, 1.50)	3.63	0.06
Tidemark	(0–4)	3.04 (2.69, 3.39)	3.80 (3.44, 4.15)	1.25	**0.003**
Average total score	*(0–31)*	*8.64 (7.07, 10.21)*	*12.92 (11.35, 14.49)*	*1.50*	***<0.001***

and Tb.N within the adjacent SAS. PTH [1-34] decreased bone surface indices (BS/BV, BS/TV) in the adjacent SBP, but increased them in the adjacent SAS.

Evaluation of osteochondral defects

Within the defects, PTH [1-34] increased thickness (Ct.Th) and mineral density (BMD) of the repaired SBP (defect SBP; Table IV) and the Tb.Th of the SAS (defect SAS), while decreasing Tb.Sp. PTH [1-34] further enhanced the connectivity of the spongious network (decreased Tb.Pf) and induced a change from a more rod-like to the native plate-like geometrical pattern (decreased SMI (1.37 vs 0.72); normal SMI: 0.74).

Evaluation of normal subchondral bone

Values of normal SBP and SAS are given in Table IV. No apparent differences were detected between adjacent SBP or SAS of operated control animals and normal SBP or SAS of non-operated animals.

Correlation between articular cartilage and subchondral bone repair

All Bland–Altman weighted correlation coefficients between the key μCT parameters BMD, BV/TV, and Ct.Th or Tb.Th from subchondral bone defects (defect SBP and SAS; Table IV) and histological average total scores of the Wakitani[27] and Sellers[28] scores (Table III) failed to attain statistical significance (all $P > 0.12$). This suggests that analysis of repair tissues at only one time point and with a small number of animals did not demonstrate time-dependent mechanisms of repair.

Discussion

The major finding of this study is that PTH [1-34] simultaneously improved the macro- and microscopic aspect of articular cartilage repair and the microarchitecture of the subchondral bone in focal osteochondral defects after 6 weeks *in vivo*. Intriguingly, these coexistent improvements of cartilage and bone repair did not correlate significantly. Of note, systemic application of PTH [1-34] directly affected the cells mediating osteochondral repair, as PTH1R expression was significantly up-regulated on the chondrocytes and osteocytes within the repair tissue. PTH [1-34] emerges therefore as a promising agent in the complex process of osteochondral repair[31], in addition to its clinically useful role to play in osteoarthritis[17,18,32] and bone repair[33–35]. This is of high significance, because there are currently no systemic therapies available to address the limited repair of focal, non-osteoarthritic osteochondral defects.

To date, only a few studies have simultaneously assessed the influence of PTH on articular cartilage and subchondral bone repair. Kudo *et al.*[19] found improved repair of focal chondral defects by intraarticular PTH [1-84] application *via* osmotic pumps but no effect on the subchondral bone as determined by histomorphometry. PTH [1-34] (10 μg/kg BW/day; 50 days) reversed osteoporotic subchondral bone changes and reduced cartilage degeneration in a rabbit model of both, osteoporosis and osteoarthritis, with the regression of cartilage damage being ascribed to an ameliorated subchondral bone support[36]. In the present study with a small sample size and only one time point investigated, the coexistent increase in bone density (BMD, BV/TV) and improvement of cartilage repair – most likely ascribed to the enhanced PTH1R expression on chondrocytes and osteocytes[37] – did not correlate significantly. However, the relatively short observation period of 6 weeks may have influenced the findings on cartilage and bone repair, as maturation of both tissues is time-dependent. Thus, extended time points are required and further investigations will be needed to elucidate whether the enhanced bone density is beneficial for long-term cartilage repair or rather reflects sclerosis, a feature of osteoarthritis.

PTH [1-34] increases BMD[14], Ct.Th[33] and Tb.Th[38], Tb.N and connectivity[34], enhancing bone strength and reducing the risk of fracture in animal models[35] and patients[14]. In a μCT evaluation of the subchondral bone in osteoporotic rabbits, Bellido *et al.*[36] found PTH [1-34] to increase the volume and thickness of cortical and

Table IV
Micro-computed tomography parameters determined in different VOIs within and adjacent to osteochondral defects. Compared to controls, PTH [1-34] application significantly increased thickness (Ct.Th) of the defect SBPBV/TV and BMD of the adjacent SBP and the microarchitecture of defect and adjacent SAS. No differences were detected between adjacent SBP or SAS of operated control animals and normal SBP or SAS of non-operated animals. Data are presented as mean values and 95% confidence intervals. BMD: bone mineral density, BV/TV: bone volume fraction, BS/BV: bone surface/volume ratio, BS/TV: bone surface density, Ct.Th: cortical thickness, Tb.Th: trabecular thickness, Tb.Sp: trabecular separation, Tb.Pf: trabecular pattern factor, Tb.N: trabecular number, SMI: structure model index, DA: degree of anisotropy, FD: fractal dimension[21], n.a.: not applicable (parameters for trabecular SAS not suitable for cortical SBP and *vice versa*). Statistical significance is highlighted by bold letters

Parameter	Unit	SBP							SAS						
		Defect SBP			Adjacent SBP			Normal SBP	Defect SAS			Adjacent SAS			Normal SAS
		PTH [1-34]	Control	*P*	PTH [1-34]	Control	*P*		PTH [1-34]	Control	*P*	PTH [1-34]	Control	*P*	
BMD	mg/cm^3	767.16 (739.05, 795.27)	720.22 (694.08, 746.36)	**0.02**	840.96 (826.62, 855.30)	741.10 (727.30, 754.90)	**<0.001**	758.22 (725.64, 790.80)	778.77 (702.67, 854.86)	704.76 (638.86, 770.66)	0.15	757.96 (730.37, 785.55)	749.86 (723.55, 776.17)	0.68	735.18 (690.60, 779.76)
BV/TV	%	50.45 (40.52, 60.39)	45.42 (36.45, 54.40)	0.46	86.51 (81.50, 91.52)	66.86 (62.02, 71.70)	**<0.001**	63.55 (57.54, 69.65)	12.55 (10.10, 15.00)	14.15 (11.83, 16.47)	0.35	22.25 (20.40, 24.10)	20.55 (18.90, 22.21)	0.18	22.70 (19.44, 25.95)
BS/BV	mm^{-1}	45.43 (36.43, 54.43)	58.19 (50.03, 66.36)	**0.04**	28.82 (26.06, 31.57)	47.85 (45.40, 50.30)	**<0.001**	44.33 (36.59, 52.08)	51.45 (47.76, 55.16)	59.08 (55.86, 62.31)	**0.01**	46.90 (44.16, 49.63)	42.77 (40.22, 45.32)	**0.03**	38.54 (34.05, 43.02)
BS/TV	mm^{-1}	22.82 (19.11, 26.52)	25.10 (21.74, 28.45)	**0.04**	23.73 (23.27, 24.19)	30.34 (29.88, 30.79)	**<0.001**	27.60 (21.83, 33.38)	6.50 (5.04, 7.95)	8.70 (7.35, 10.05)	**0.03**	10.50 (9.91, 11.09)	8.53 (8.01, 9.05)	**0.001**	7.79 (6.45, 9.13)
Ct.Th	mm	0.25 (0.22, 0.27)	0.19 (0.17, 0.22)	**0.01**	0.36 (0.34, 0.38)	0.23 (0.21, 0.25)	**<0.001**	0.25 (0.22, 0.27)	n.a.	n.a.		n.a.	n.a.		n.a.
Tb.Th	mm	n.a.	n.a.		n.a.	n.a.		n.a.	0.08 (0.07, 0.08)	0.06 (0.06, 0.06)	**0.01**	0.09 (0.08, 0.09)	0.07 (0.07, 0.08)	**0.01**	0.08 (0.06, 0.10)
Tb.Sp	mm	n.a.	n.a.		n.a.	n.a.		n.a.	0.46 (0.38, 0.55)	0.78 (0.70, 0.85)	**0.01**	0.33 (0.31, 0.35)	0.38 (0.36, 0.40)	**0.001**	0.41 (0.34, 0.47)
Tb.Pf	mm^{-1}	n.a.	n.a.		n.a.	n.a.		n.a.	−4.90 (−9.22, −0.58)	3.87 (−0.05, 7.81)	**0.01**	−3.43 (−8.11, 1.26)	−3.95 (−8.21, 0.31)	0.87	−4.48 (−5.62, −3.34)
Tb.N	mm^{-1}	n.a.	n.a.		n.a.	n.a.		n.a.	1.75 (1.33, 2.16)	2.17 (1.78, 2.55)	0.15	2.85 (2.71, 2.99)	2.31 (2.17, 2.45)	**0.001**	2.15 (2.05, 2.24)
SMI	−/−	n.a.	n.a.		n.a.	n.a.		n.a.	0.72 (0.38, 1.06)	1.39 (1.08, 1.71)	**0.01**	0.46 (0.06, 0.85)	0.54 (0.18, 0.90)	0.75	0.74 (0.28, 1.20)
DA	−/−	n.a.	n.a.		n.a.	n.a.		n.a.	0.66 (0.61, 0.70)	0.65 (0.61, 0.69)	0.80	0.47 (0.46, 0.49)	0.49 (0.48, 0.51)	0.52	0.55 (0.42, 0.68)
FD	−/−	n.a.	n.a.		n.a.	n.a.		n.a.	2.34 (2.28, 2.39)	2.30 (2.25, 2.35)	0.30	2.28 (2.25, 2.32)	2.31 (2.28, 2.34)	0.30	2.32 (2.32, 2.32)

trabecular subchondral bone. These results are in good agreement with the present study in which PTH [1-34] exerted its effects on both, the SBP and the SAS, yielding a larger area of reconstituted subchondral bone in the treatment group while control defects were still repairing at 6 weeks. However, the effects of PTH [1-34] on the subchondral bone are not necessarily an improvement, but may also indicate the initiation of osteoarthritis[39,40]. Remarkably, this impact on the osseous microarchitecture was accompanied by an increase in serum levels of calcium and AP.

Apart from the well-documented anabolic effects of PTH [1-34] on bone, its *in vivo* impact on articular cartilage is seldom described. For osteoarthritis, Chang *et al.*[18] and Sampson *et al.*[17] have shown that PTH [1-34] may inhibit the progress of cartilage degeneration in rat or mouse knees after 5 or 12 weeks *in vivo*, respectively. The negative correlation between PTH1R expression and the histological grading of lapine osteoarthritic cartilage[32] may explain this finding. Kudo *et al.* studied the effect of intraarticular administration of human PTH [1-84] on full-thickness chondral defects in the rabbit trochlea. Although the treatment induced articular cartilage repair – possibly by enhancing mesenchymal cell proliferation[19] – it inhibited chondrogenic differentiation of progenitor cells[41]. Feeley *et al.*[42] even described a deleterious effect of 10 μg PTH [1-34]/kg BW/day (over 1 or 4 weeks) on the histological characteristics of cartilage repair three months after microfracture treatment of 6 mm chondral defects in rabbits. In the present study, the same dose improved the macroscopic appearance and the overall histological grading of the cartilage repair tissue in two scoring systems[27,28] with a high inter-score correlation ($r = 0.98$). However, the immunoreactivity of the repair tissues to type-I and type-II collagen remained unaffected by PTH [1-34], possibly because either maximum collagen expression was already achieved or differentiation of the repair tissue (type-II collagen deposition *vis-à-vis* type-I collagen reduction) had not yet commenced after 6 weeks *in vivo*. Besides, the biochemical composition of the repair tissue remained unchanged. Notably, this supports our previous finding that histological and biochemical parameters of articular cartilage repair do not correlate[29]. PTH [1-34] induced neither proliferation of cells repopulating the defects (unchanged DNA concentrations and total cell numbers; Table II), neither apoptosis of chondrocytes and osteocytes, and the reported percentages of apoptotic chondrocytes and osteocytes are in good agreement with literature values[43,44]. Further, the treatment did not yield degenerative changes in the adjacent cartilage or an inflammatory response in the synovial membrane. This is of clinical importance, as synovialitis contributes to cartilage degeneration[45].

The significantly up-regulated expression of PTH1R on osteocytes within the repaired subchondral bone and chondrocytes within the cartilaginous repair tissue indicates that systemic application of PTH [1-34] was capable of directly stimulating these local cells. Both, articular chondrocytes[11] and osteocytes[10] express PTH1R, and binding of PTH [1-34] to its receptor[46] may enhance the expression and production of growths factors with downstream effect on their antagonists[47].

The dosage of PTH [1-34] varies considerably among experimental investigations[35]. Here, 10 μg PTH [1-34]/kg BW/day[16] were chosen because metaphyseal bone healing of rabbits[48] was improved by the same dose over 4 weeks. While intermittent and short-term stimulation of PTH [1-34] favors bone formation in animals[49] and patients[14], a higher dosage (40 μg/kg BW/day for 20 weeks)[50] or persistently high levels induce a significant loss in animal BW and increased serum calcium and AP concentration.

In conclusion, systemic administration of PTH [1-34] simultaneously stimulates articular cartilage and subchondral bone repair in focal osteochondral defects. PTH [1-34] therefore emerges as an important therapeutic treatment option in the complex process of osteochondral repair.

Author contributions

Conception and design: PO, MC, HM.
Obtaining of funding: HM.
Collection and assembly of data: PO, MC, MDM, HM.
Analysis and interpretation of the data: PO, MC, DZ, MDM, DMK, HM.
Statistical expertise: PO, MC, DZ, HM.
Article drafting and revision: PO, MC, DZ, MDM, DMK, HM.
Final approval of the article: PO, MC, DZ, MDM, DMK, HM.

Role of funding source

Financial support was received from the Center of Experimental Orthopaedics, Homburg/Saar, Germany. The sponsor was not involved in the study design, data collection or analysis or in the writing of the manuscript. Furthermore, they did not influence the decision to submit the manuscript for publication.

Competing interest statement

The authors have no conflicts of interest to disclose.

Acknowledgments

We thank E. Kabiljagic for expert technical assistance during the animal experiments. We also thank G. Schmitt, V. Just, and J. Becker for assistance in histological processing.

References

1. Orth P, Cucchiarini M, Kaul G, Ong MF, Gräber S, Kohn DM, *et al.* Temporal and spatial migration pattern of the subchondral bone plate in a rabbit osteochondral defect model. Osteoarthritis Cartilage 2012;20(10):1161–9.
2. Lajeunesse D. The role of bone in the treatment of osteoarthritis. Osteoarthritis Cartilage 2004;12(Suppl A):S34–8.
3. Madry H, van Dijk CN, Mueller-Gerbl M. The basic science of the subchondral bone. Knee Surg Sports Traumatol Arthrosc 2010;18(4):419–33.
4. Gomoll AH, Farr J, Gillogly SD, Kercher J, Minas T. Surgical management of articular cartilage defects of the knee. J Bone Joint Surg Am 2010;92(14):2470–90.
5. Hangody L, Kish G, Karpati Z, Udvarhelyi I, Szigeti I, Bely M. Mosaicplasty for the treatment of articular cartilage defects: application in clinical practice. Orthopedics 1998;21(7):751–6.
6. Ochs BG, Muller-Horvat C, Albrecht D, Schewe B, Weise K, Aicher WK, *et al.* Remodeling of articular cartilage and subchondral bone after bone grafting and matrix-associated autologous chondrocyte implantation for osteochondritis dissecans of the knee. Am J Sports Med 2011;39(4):764–73.
7. Brittberg M. Autologous chondrocyte implantation-technique and long-term follow-up. Injury 2008;39(Suppl 1):S40–9.
8. Matricali GA, Dereymaeker GP, Luyten FP. Donor site morbidity after articular cartilage repair procedures: a review. Acta Orthop Belg 2010;76(5):669–74.
9. von Rechenberg B, Akens MK, Nadler D, Bittmann P, Zlinszky K, Kutter A, *et al.* Osteochondral grafts. Osteoarthritis Cartilage 2003;11(4):265–77.
10. Rhee Y, Allen MR, Condon K, Lezcano V, Ronda AC, Galli C, *et al.* PTH receptor signaling in osteocytes governs periosteal bone formation and intracortical remodeling. J Bone Miner Res 2011;26(5):1035–46.

11. Weisser J, Riemer S, Schmidl M, Suva LJ, Poschl E, Brauer R, *et al*. Four distinct chondrocyte populations in the fetal bovine growth plate: highest expression levels of PTH/PTHrP receptor, Indian hedgehog, and MMP-13 in hypertrophic chondrocytes and their suppression by PTH (1-34) and PTHrP (1-40). Exp Cell Res 2002;279(1):1–13.
12. Bukata SV. Systemic administration of pharmacological agents and bone repair: what can we expect. Injury 2011; 42(6):605–8.
13. Bukata SV, Puzas JE. Orthopedic uses of teriparatide. Curr Osteoporos Rep 2010;8(1):28–33.
14. Neer RM, Arnaud CD, Zanchetta JR, Prince R, Gaich GA, Reginster JY, *et al*. Effect of parathyroid hormone (1-34) on fractures and bone mineral density in postmenopausal women with osteoporosis. N Engl J Med 2001;344(19):1434–41.
15. Kakar S, Einhorn TA, Vora S, Miara LJ, Hon G, Wigner NA, *et al*. Enhanced chondrogenesis and Wnt signaling in PTH-treated fractures. J Bone Miner Res 2007;22(12):1903–12.
16. O'Loughlin PF, Cunningham ME, Bukata SV, Tomin E, Poynton AR, Doty SB, *et al*. Parathyroid hormone (1-34) augments spinal fusion, fusion mass volume, and fusion mass quality in a rabbit spinal fusion model. Spine (Phila Pa 1976) 2009;34(2):121–30.
17. Sampson ER, Hilton MJ, Tian Y, Chen D, Schwarz EM, Mooney RA, *et al*. Teriparatide as a chondroregenerative therapy for injury-induced osteoarthritis. Sci Transl Med 2011;3(101):101ra93.
18. Chang JK, Chang LH, Hung SH, Wu SC, Lee HY, Lin YS, *et al*. Parathyroid hormone 1-34 inhibits terminal differentiation of human articular chondrocytes and osteoarthritis progression in rats. Arthritis Rheum 2009;60(10):3049–60.
19. Kudo S, Mizuta H, Takagi K, Hiraki Y. Cartilaginous repair of full-thickness articular cartilage defects is induced by the intermittent activation of PTH/PTHrP signaling. Osteoarthritis Cartilage 2011;19(7):886–94.
20. Goebel L, Orth P, Müller A, Zurakowski D, Bücker A, Cucchiarini M, *et al*. Experimental scoring systems for macroscopic articular cartilage repair correlate with the MOCART score assessed by a high-field MRI at 9.4 T – comparative evaluation of five macroscopic scoring systems in a large animal cartilage defect model. Osteoarthritis Cartilage 2012;20(9):1046–55.
21. Feldkamp LA, Goldstein SA, Parfitt AM, Jesion G, Kleerekoper M. The direct examination of three-dimensional bone architecture in vitro by computed tomography. J Bone Miner Res 1989;4(1):3–11.
22. Weimer A, Madry H, Venkatesan JK, Schmitt G, Frisch J, Wezel A, *et al*. Benefits of rAAV-mediated IGF-I overexpression for the long-term reconstruction of human osteoarthritic cartilage by modulation of the IGF-I axis. Mol Med 2012;18(1): 346–58.
23. Kiernan JA. Histological and Histochemical Methods – Theory and Practice. Oxford: Butterworth-Heinemann; 1999.
24. Fortier LA, Mohammed HO, Lust G, Nixon AJ. Insulin-like growth factor-I enhances cell-based repair of articular cartilage. J Bone Joint Surg Br 2002;84(2):276–88.
25. Madry H, Kaul G, Cucchiarini M, Stein U, Zurakowski D, Remberger K, *et al*. Enhanced repair of articular cartilage defects in vivo by transplanted chondrocytes overexpressing insulin-like growth factor I (IGF-I). Gene Ther 2005;12(15): 1171–9.
26. Laverty S, Girard CA, Williams JM, Hunziker EB, Pritzker KP. The OARSI histopathology initiative – recommendations for histological assessments of osteoarthritis in the rabbit. Osteoarthritis Cartilage 2010;18(Suppl 3):S53–65.
27. Wakitani S, Goto T, Pineda SJ, Young RG, Mansour JM, Caplan AI, *et al*. Mesenchymal cell-based repair of large, full-thickness defects of articular cartilage. J Bone Joint Surg Am 1994;76(4):579–92.
28. Sellers RS, Peluso D, Morris EA. The effect of recombinant human bone morphogenetic protein-2 (rhBMP-2) on the healing of full-thickness defects of articular cartilage. J Bone Joint Surg Am 1997;79(10):1452–63.
29. Orth P, Zurakowski D, Wincheringer D, Madry H. Reliability, reproducibility, and validation of five major histological scoring systems for experimental articular cartilage repair in the rabbit model. Tissue Eng Part C Methods 2012;18(5):329–39.
30. Bland JM, Altman DG. Calculating correlation coefficients with repeated observations: part 2 – correlation between subjects. BMJ 1995;310(6980):633.
31. Goldring MB, Marcu KB. Cartilage homeostasis in health and rheumatic diseases. Arthritis Res Ther 2009;11(3):224.
32. Becher C, Szuwart T, Ronstedt P, Ostermeier S, Skwara A, Fuchs-Winkelmann S, *et al*. Decrease in the expression of the type 1 PTH/PTHrP receptor (PTH1R) on chondrocytes in animals with osteoarthritis. J Orthop Surg Res 2010;5:28.
33. Dempster DW, Cosman F, Kurland ES, Zhou H, Nieves J, Woelfert L, *et al*. Effects of daily treatment with parathyroid hormone on bone microarchitecture and turnover in patients with osteoporosis: a paired biopsy study. J Bone Miner Res 2001;16(10):1846–53.
34. Brouwers JE, van Rietbergen B, Huiskes R, Ito K. Effects of PTH treatment on tibial bone of ovariectomized rats assessed by in vivo micro-CT. Osteoporos Int 2009;20(11):1823–35.
35. Ellegaard M, Jorgensen NR, Schwarz P. Parathyroid hormone and bone healing. Calcif Tissue Int 2010;87(1):1–13.
36. Bellido M, Lugo L, Roman-Blas JA, Castaneda S, Calvo E, Largo R, *et al*. Improving subchondral bone integrity reduces progression of cartilage damage in experimental osteoarthritis preceded by osteoporosis. Osteoarthritis Cartilage 2011;19(10): 1228–36.
37. Anraku Y, Mizuta H, Sei A, Kudo S, Nakamura E, Senba K, *et al*. Analyses of early events during chondrogenic repair in rat full-thickness articular cartilage defects. J Bone Miner Metab 2009;27(3):272–86.
38. Novince CM, Entezami P, Wilson CG, Wang J, Oh S, Koh AJ, *et al*. Impact of proteoglycan-4 and parathyroid hormone on articular cartilage. J Orthop Res 2012 Aug 15 [Epub ahead of print].
39. Goldring MB, Goldring SR. Articular cartilage and subchondral bone in the pathogenesis of osteoarthritis. Ann N Y Acad Sci 2010;1192:230–7.
40. Henrotin Y, Pesesse L, Sanchez C. Subchondral bone in osteoarthritis physiopathology: state-of-the art and perspectives. Biomed Mater Eng 2009;19(4–5):311–6.
41. Kudo S, Mizuta H, Otsuka Y, Takagi K, Hiraki Y. Inhibition of chondrogenesis by parathyroid hormone in vivo during repair of full-thickness defects of articular cartilage. J Bone Miner Res 2000;15(2):253–60.
42. Feeley BT, Doty SB, Devcic Z, Warren RF, Lane JM. Deleterious effects of intermittent recombinant parathyroid hormone on cartilage formation in a rabbit microfracture model: a preliminary study. HSS J 2010;6(1):79–84.
43. Lee JH, Prakash KV, Pengatteeri YH, Park SE, Koh HS, Han CW. Chondrocyte apoptosis in the regenerated articular cartilage after allogenic chondrocyte transplantation in the rabbit knee. J Bone Joint Surg Br 2007;89(7):977–83.
44. Jaiprakash A, Prasadam I, Feng JQ, Liu Y, Crawford R, Xiao Y. Phenotypic characterization of osteoarthritic osteocytes from the sclerotic zones: a possible pathological role in subchondral bone sclerosis. Int J Biol Sci 2012;8(3):406–17.

45. Lugo L, Villalvilla A, Gómez R, Bellido M, Sánchez-Pernaute O, Largo R, *et al*. Effects of PTH [1-34] on synoviopathy in an experimental model of osteoarthritis preceded by osteoporosis. Osteoarthritis Cartilage 2012;20(12):1619–30.
46. Coleman DT, Bilezikian JP. Parathyroid hormone stimulates formation of inositol phosphates in a membrane preparation of canine renal cortical tubular cells. J Bone Miner Res 1990;5(3):299–306.
47. Wang Y, Nishida S, Boudignon BM, Burghardt A, Elalieh HZ, Hamilton MM, *et al*. IGF-I receptor is required for the anabolic actions of parathyroid hormone on bone. J Bone Miner Res 2007;22(9):1329–37.
48. Tsiridis E, Morgan EF, Bancroft JM, Song M, Kain M, Gerstenfeld L, *et al*. Effects of OP-1 and PTH in a new experimental model for the study of metaphyseal bone healing. J Orthop Res 2007;25(9):1193–203.
49. Hock JM, Gera I. Effects of continuous and intermittent administration and inhibition of resorption on the anabolic response of bone to parathyroid hormone. J Bone Miner Res 1992;7(1):65–72.
50. Hirano T, Burr DB, Turner CH, Sato M, Cain RL, Hock JM. Anabolic effects of human biosynthetic parathyroid hormone fragment (1-34), LY333334, on remodeling and mechanical properties of cortical bone in rabbits. J Bone Miner Res 1999;14(4):536–45.